

# Controlled Torsional Deformation by Swelling a Hyperelastic Cylinder with Helically Wound Fibers

## Abstract

The combined effect of radial deformation and torsion is examined for a transversely isotropic hyperelastic cylindrical tube when it is subject to finite deformation swelling. We consider a specific strain energy function that models fibers that do not swell within a matrix that expands by swelling. We solve a boundary value problem for a tube with a single family of fibers that are wound about the tube in a helical fashion. An imposed swelling field then gives a torsional deformation. The analysis shows how the twist increases with swelling and predicts an asymptotic value of twist as the swelling becomes arbitrarily large. To test these predictions a fiber-reinforced actuator device capable of torsional motion is constructed. The anisotropy is achieved by incorporating thin platinum wires into a conjugated polymer matrix material. The actuator performance is modeled by using the finite elasticity based theory and the results are compared with the experimental data.

## Keywords

Swelling — Torsion — Fiber Reinforcement — Nonlinear Elasticity — Actuators — Conjugated Polymer

**Hasan DEMIRKOPARAN**, Carnegie Mellon University in Qatar, hasand@qatar.cmu.edu

**Yang FANG**, Advanced Bionics, Valencia, California, yfang.msu@gmail.com

**Thomas J. PENCE**, Michigan State University, Department of Mechanical Engineering, pence@egr.msu.edu

**Xiaobo TAN**, Michigan State University, Smart Microsystems Laboratory, xbtan@egr.msu.edu

## Introduction

Fiber reinforced elastic materials can deform in a complicated fashion when they swell. Normally this is a small effect. However if the swelling is large, and if the fibers and matrix exhibit differential swelling, then the resulting constraint stresses can lead to complicated patterns of deformation. Indeed certain aspects of plant motion are controlled by such a swelling effect. This phenomenon can also be exploited to create devices that exhibit complex modes of deformation. To obtain such modes, and to control their activation, it is necessary to consider specifically designed fiber arrangements. Given a deformation mode the determination of the necessary fiber geometry is an interesting inverse problem. To demonstrate the possibilities for the creation of such devices, we here focus on torsional deformations that are achieved by the swelling of a tube that contains a single family of helically wound fibers. If the fibers exhibit negligible swelling, then the offsetting tendencies of a matrix that wants to expand and a family of fibers that wants to maintain its natural stress-free length leads to a compromise deformation in which the tube twists in a torsional mode. To demonstrate these effects a simple device has been constructed that consists of platinum wires embedded in a conjugated polymer matrix that in turn is immersed in solution. Upon application of a voltage, the matrix swells due to ionic uptake and the resulting deformation closely replicates the theoretical prediction. Here we report on the most basic aspects. Full details can be found in [1] and [2].

## 1. Torsional Swelling of a Hyperelastic Tube

We consider a hollow tube whose initial configuration is given by

$$\Omega_X = \{(R, \Theta, Z) : R_i \leq R \leq R_o, 0 \leq \Theta < 2\pi, 0 \leq Z \leq L\} \quad (1)$$

where  $R_o > R_i > 0$  and  $L > 0$ . Let  $e_R, e_\Theta, e_Z$  be the set of orthonormal unit vectors in a polar coordinate system for this configuration. Let  $\mathbf{M}$  be a unit vector in the above initial configuration that defines a single direction of fiber reinforcement. It is assumed that the fibers are wound around the tube in a helical fashion such that they make a pitch angle  $\beta$  with respect to the axis of the tube. Hence

$$\mathbf{M} = \sin \beta e_\Theta + \cos \beta e_Z \quad (2)$$

with  $0 < \beta < \pi/2$ . Torsional deformations are described in a polar coordinate description by relations of the form

$$r = r(R), \quad \theta = \Theta + \kappa Z, \quad z = \lambda_z Z \quad (3)$$

where  $r(R)$  is an unknown function to be determined;  $\kappa$  and  $\lambda_z$  are constants. The constant  $\kappa$  is the twist per unit length

and the constant  $\lambda_z$  is the elongation per unit length in the longitudinal direction.

Deformations of this type are viewed as maps from a material point at  $\mathbf{X}$  to a new location  $\mathbf{y}$  in the deformed configuration. The deformation gradient tensor  $\mathbf{F} = \partial \mathbf{y} / \partial \mathbf{X}$  for the deformation (3) is

$$\mathbf{F} = r' e_r \otimes e_R + \frac{r}{R} e_\theta \otimes e_\Theta + \kappa r e_\theta \otimes e_Z + \lambda_z e_z \otimes e_Z \quad (4)$$

where  $r' = dr / dR$ . Here  $\{e_r, e_\theta, e_z\}$  is the unit orthonormal basis in polar coordinates for the deformed configuration. We consider situations where the natural free volume  $v$  is controllable. An example, as discussed later, is the conjugate polymer actuator that has been built. The specification of the natural free volume provides the condition

$$\det \mathbf{F} = v. \quad (5)$$

It is to be remarked that  $v$  is the natural free volume with respect to the reference configuration. Since  $v$  is controllable it is regarded as a given quantity. The following analysis applies to a case in which  $v$  may depend upon  $R$  but is independent of  $\Theta$  and  $Z$ . Note that from (4) and (5) it follows that

$$\frac{1}{R} \lambda_z r \frac{dr}{dR} = v. \quad (6)$$

Let  $r_i = r(R_i)$  and  $r_o = r(R_o)$ . Then upon integration Equation (6) gives

$$r^2 = r_i^2 + \frac{2}{\lambda_z} \int_{R_i}^R v(R) R dR. \quad (7)$$

It is to be remarked that once  $\lambda_z$  and  $v(R)$  have been specified then the value  $r_i$  in Equation (7) completely determines the mapping between  $R$  and  $r$ .

### 1.1 Material Model

The tube is modeled as being an anisotropic hyperelastic material. The anisotropy is chosen so as to model the effect of the fibers. Specifically, the stored energy density  $W$  of the material is taken to be given by

$$W = \Phi_m(I_1, v) + \Phi_f(I_4). \quad (8)$$

Here  $I_1$  is the first invariant of the left Cauchy-Green deformation tensor  $\mathbf{B} = \mathbf{F} \mathbf{F}^T$  which is defined by  $I_1 = \text{tr}(\mathbf{B})$ , and  $I_4 = \mathbf{F} \mathbf{M} \cdot \mathbf{F} \mathbf{M}$  is the square of the stretch experienced by the reinforcing fibers. Moreover  $\Phi_m$  and  $\Phi_f$  are the elastic energy density for the matrix and the associated fiber family. Form (8) provides a simple model for an isotropic swelling matrix with nonswelling fibers and details can be found in [1].

Note from Equations (2) and (4) that  $I_1$  and  $I_4$  are given by

$$I_1 = \frac{v^2 R^2}{\lambda_z^2 r^2} + \frac{r^2}{R^2} + \kappa^2 r^2 + \lambda_z^2, \quad (9)$$

$$I_4 = \left( \kappa \cos \beta + \frac{1}{R} \sin \beta \right)^2 r^2 + \lambda_z^2 \cos^2 \beta. \quad (10)$$

The Cauchy stress tensor for such a swelling material is given by

$$\boldsymbol{\sigma} = \frac{1}{v} \frac{\partial W}{\partial \mathbf{F}} \mathbf{F}^T - p \mathbf{I} \quad (11)$$

where  $\mathbf{I}$  is the identity tensor and  $p = p(v)$  is the (unknown) hydrostatic pressure associated with the constraint (5). The Cauchy stress is required to satisfy the equilibrium equation

$$\text{div} \boldsymbol{\sigma} = 0, \quad (12)$$

whereupon it is found that the  $\theta$  and  $z$  component equations give that the pressure is a function of  $r$  only. The inner and outer surfaces of the tube are taken to be traction free, and so give boundary conditions in the form:

$$\boldsymbol{\sigma}_{rr} \Big|_{R=R_o} = 0, \quad \boldsymbol{\sigma}_{rr} \Big|_{R=R_i} = 0. \quad (13)$$

The equilibrium equation in the  $e_r$  direction becomes

$$\frac{dp}{dR} = \frac{vR}{\lambda_z r^2} (\boldsymbol{\sigma}_{rr} - \boldsymbol{\sigma}_{\theta\theta}) + \frac{2}{\lambda_z} \frac{d}{dR} \left( \frac{v(R) R^2}{r^2} \Phi'_m(I_1, v(R)) \right) \quad (14)$$

where  $\Phi'_m = \partial \Phi_m / \partial I_1$ .

The elastic energy density of the matrix will be taken in the modified neo-Hookean form:

$$\Phi_m(I_1, v) = \frac{\mu}{2} (I_1 - 3v^{2/3}) \quad (15)$$

where  $\mu$  is a material constant. The strain energy function for the fiber component will be taken as

$$\Phi_f(I_4) = \frac{\gamma}{2} (I_4 - 1)^2, \quad (16)$$

where  $\gamma$  is another material constant. The ratio  $\gamma/\mu$  is indicative of the fiber stiffness relative to the matrix stiffness.

The radial and azimuthal normal stress components of the Cauchy stress tensor can be calculated from Equation (11) and then Equation (14) can be integrated to obtain the following form of  $p$  by using the boundary condition  $\boldsymbol{\sigma}_{rr} \Big|_{R=R_o} = 0$ :

$$\begin{aligned}
 p = \frac{\nu R^2 \mu}{\lambda_z^2 r^2} - \mu \int_R^{R_o} \frac{\nu^2 R^3}{\lambda_z^3 r^4} - \frac{R^2 \kappa^2 + 1}{\lambda_z R} dR \\
 - \gamma \int_R^{R_o} \frac{2R}{\lambda_z} \left( \kappa \cos \beta + \frac{1}{R} \sin \beta \right)^2 (I_4 - 1) dR.
 \end{aligned} \quad (17)$$

The other boundary condition  $\sigma_{rr}|_{R=R_i} = 0$  in conjunction with Equation (17) gives the following requirement:

$$\begin{aligned}
 \frac{\mu}{2} \int_{R_i}^{R_o} \left( -\frac{\nu^2 R^2}{\lambda_z^2 r^4} + \kappa^2 + \frac{1}{R^2} \right) R dR \\
 + \gamma \int_{R_i}^{R_o} \left( \kappa \cos \beta + \frac{1}{R} \sin \beta \right)^2 (I_4 - 1) R dR = 0.
 \end{aligned} \quad (18)$$

For a given  $\kappa$ ,  $\lambda_z$  and  $\nu(R)$ , Equation (18) serves to determine the previously unknown value  $r_i$ .

## 1.2 Torque-free Torsion

Consider tubes for which there is no restraining external torque applied on either end. Such a torque or twisting moment  $T$  is given by

$$T = 2\pi \int_{r_i}^{r_o} \sigma_{\theta z} r^2 dr. \quad (19)$$

For a given  $\lambda_z$  and  $\nu(R)$ , Equation (18) and the condition  $T=0$  with  $T$  given by Equation (19) serves to determine both  $r_i$  and the twist per unit length  $\kappa$ . For the material with stored energy densities given by (15) and (16) the shear stress appearing in the integral (19) takes the form

$$\sigma_{\theta z} = \frac{\mu}{\nu} \kappa \lambda_z r + \frac{2\gamma}{\nu} \lambda_z r \cos \beta \left( \kappa \cos \beta + \frac{1}{R} \sin \beta \right) (I_4 - 1) \quad (20)$$

As an example consider swelling that is independent of  $R$ , and geometric and material parameter choices as follows:  $R_i = 2.2$  mm,  $R_o = 2.581$  mm,  $\mu = 80$  MPa, and  $\gamma = 34$  GPa. For such a tube, consider two different fiber orientations:  $\beta = 60^\circ$  and  $\beta = 80^\circ$ . In each case consider the three possible values of axial stretch  $\lambda_z$  as follows: 0.9, 1.0, and 1.1. Then solution of the two equations for and the two unknowns  $r_i$  and  $\kappa$  as a function of  $\nu$  gives graphs as shown in Figures 1 – 4. It is to be noted that decreasing stretch  $\lambda_z$  gives rise to an increased value of inner radius  $r_i$  and also to an increased magnitude of twist per unit length  $|\kappa|$  for all parameter values under consideration.

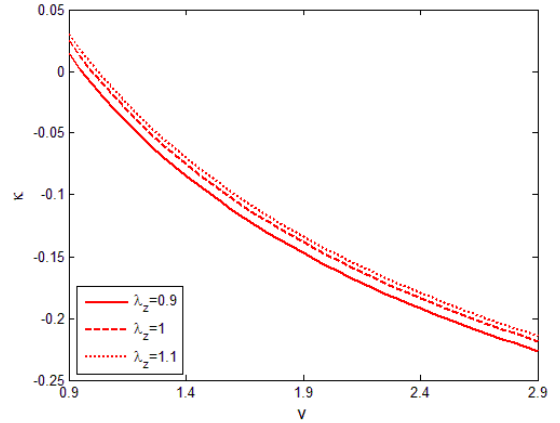


**Figure 1.** Graph of the twist per unit length  $\kappa$  versus swelling  $\nu$  for selected  $\lambda_z$  values. Here  $R_i = 2.2$  mm,  $R_o = 2.581$  mm,  $\beta = 60^\circ$ ,  $\mu = 80$  MPa, and  $\gamma = 34$  GPa.

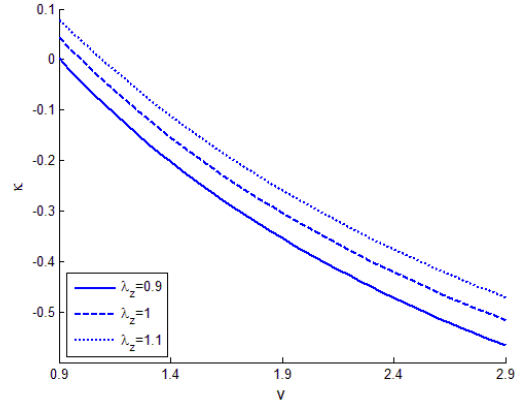


**Figure 2.** Graph of the twist per unit length  $\kappa$  versus swelling  $\nu$  for selected  $\lambda_z$  values. Here  $R_i = 2.2$  mm,  $R_o = 2.581$  mm,  $\beta = 80^\circ$ ,  $\mu = 80$  MPa, and  $\gamma = 34$  GPa.

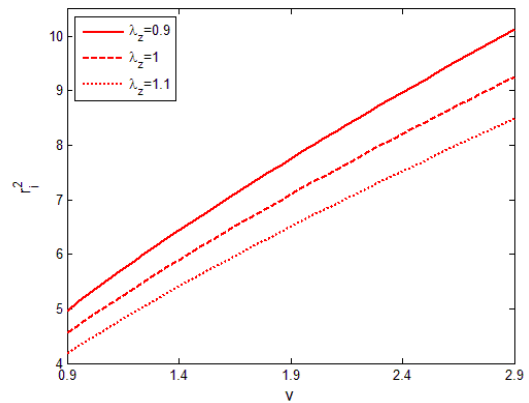


**Figure 3.** Graph of  $r_i^2$  versus swelling  $\nu$  for selected  $\lambda_z$  values. Here  $R_i = 2.2$  mm,  $R_o = 2.581$  mm,  $\beta = 60^\circ$ ,  $\mu = 80$  MPa, and  $\gamma = 34$  GPa.

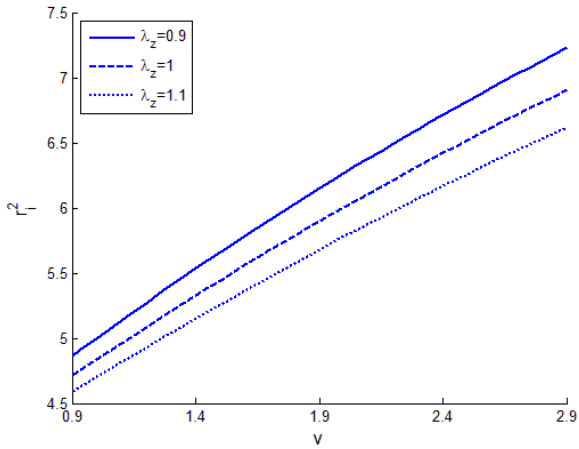


**Figure 4.** Graph of  $r_i^2$  versus swelling  $\nu$  for selected  $\lambda_z$  values. Here  $R_i = 2.2$  mm,  $R_o = 2.581$ mm,  $\beta = 80^\circ$ ,  $\mu = 80$  MPa, and  $\gamma = 34$  GPa.

For very large swelling the value of  $\kappa$  approaches an asymptotic value  $\kappa_\infty$  that is obtained as the root of a cubic equation. For the parameter values associated with Figures 2 and 4 this root is found to be  $\kappa_\infty = -2.30222 / \text{mm}$ . In general the fibers change their orientation to the direction **FM**. For very large swelling this reorientation gives rise to a localized internal layer of rapid variation in deformed fiber orientation. In the infinite swelling limit this layer collapses onto a single radius value at which the fibers abruptly change their orientation by  $180^\circ$  (Figure 5). Inside this special radius the deformed fibers exhibit circumferential orientation in the original winding sense. Outside this special radius the fibers exhibit circumferential orientation in the opposite winding sense.

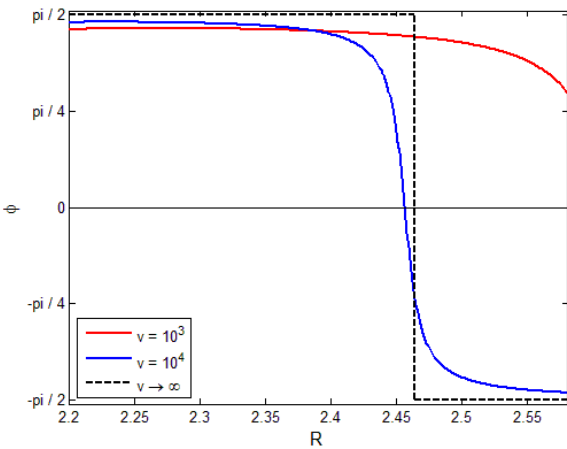


**Figure 5.** Graph of  $\phi$  versus  $R$  for selected  $\nu$  values. Here  $\phi$  is the angle that the fibers make with  $z$ -axis after the deformation. Here  $\lambda_z = 1$ ,  $R_i = 2.2$  mm,  $R_o = 2.581$ mm,  $\beta = 80^\circ$ ,  $\mu = 80$  MPa, and  $\gamma = 34$  GPa.

## 2. Fiber-reinforced Conjugated Polymer Torsional Actuator

Conjugated polymers have physical properties conducive to the construction of devices for sensing and actuating. As these polymers have alternating single and

double carbon-carbon bonds, when placed in ionic solution and stripped of electrons such polymers will absorb negative ions. The transportation of these anions in and out of the polymer matrix can thus be obtained by creating an electrical potential difference. The additional free volume supplied by the anions show how a volumetric change is induced in the polymer matrix by supplying a voltage. Further, the stability of these anions within the matrix under such electrical control motivates the condition of volume specification which is given in Equation (5).

### 2.1 Fabrication Process

To demonstrate, a torsional actuator has been fabricated by helically embedding platinum fibers into a polypyrrole (PPy) tube. Details of the fabrication procedure can be found in Fang et al. [2]. The strains produced by PPy actuators are typically between 1% and 10% [3], [4]. Moreover a 20% contraction in the thickness direction of a polyaniline film has also been reported [5]. Such strains are beyond those that are appropriate for a linear elasticity based treatment, consequently the nonlinear elasticity based model of the type considered here is more suitable for describing the deformation experienced by any such conjugated-polymer actuator.

By applying a voltage difference between the fiber-reinforced PPy tube and an auxiliary electrode that is placed at a separate location in the electrolyte, negatively charged ions can be forced to move in (or out) of the PPy tube. As a result of this transportation, the tube swells (or deswells). This transportation initiates a mechanical interaction between the PPy swellable matrix and the nonswelling fibers as the fibers seek to maintain their natural length. This mechanical interaction is governed by Equation (12).

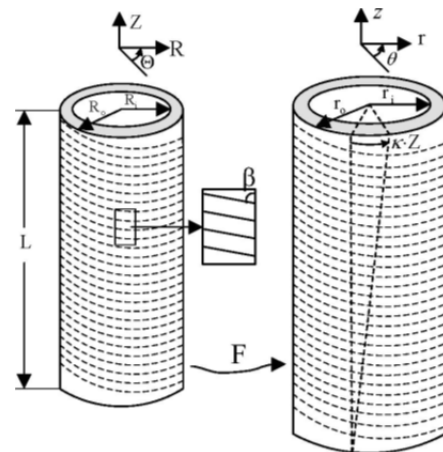


**Figure 6.** Illustration of the tube before and after the deformation

### 2.2 Experimental Setup

Four fiber-reinforced PPy actuators were fabricated according to such a specification. The tube is characterized by three geometric parameters; its inner radius  $R_i$ , thickness  $t$  (the difference

between outer radius and inner radius), and the fiber winding pitch angle  $\beta$ . Because the length  $L$  of the tube is large in comparison to the other geometric parameters, end effects can be assumed small so that the resultant  $T = 0$  condition can replace a pointwise boundary condition in terms of shear tractions.

The values of the geometric parameters for the four samples are listed in the following Table:

**Table 1.** Geometric Parameters for Four Sample Actuators Used in Experiments

	Thickness (mm)	pitch angle	radius (mm)
Sample 1	0.381	80	2.2
Sample 2	0.381	80	1.3
Sample 3	0.686	60	2.2
Sample 4	0.686	60	2.2

Consider the properties of the PPy matrix and the platinum wires. The wire radii, stiffness, and volume density within the PPy matrix gives rise to an effective modulus value of  $\gamma = 34$  GPa with respect to the original reference volume. In a similar fashion, the matrix material properties in conjunction with its volume fraction leads to a value of  $\mu = 80$  MPa for the PPy matrix. This accounts for the parameter choices that are made with respect to the Figures 1 – 4. In particular, Figures 2 and 4 correspond directly to parameter choices representative of Actuator Sample 1.

### 2.3 Experimental Setup to Measure the Deformation Parameters

There are three variables that characterize the deformation of the actuator: the inner radius  $r_i$ , the twist per unit length  $\kappa$ , and the elongation per unit length  $\lambda_z$ . During the experiments these three quantities are measured directly. The inner radius  $r_i$  is determined by caliper measurement. The elongation per unit length  $\lambda_z$  is also immediate by linear measurement of the elongation for the swollen tube as compared to the known original length. To obtain  $\kappa$ , a laser sensor was used to determine the displacement of a copper film that was attached to the outer surface of the tube. Prior to actuation, the laser was situated so as to make a right angle with the film. Let  $R_m$  be the distance between the center of the tube and the incident point for the laser upon the film. When actuated, the measured displacement  $y$  of the laser's new incident point is related to  $\kappa$  via  $y = R_m \tan(\kappa L)$ . Figure 7 provides a schematic of the calibrated laser measurement scheme.

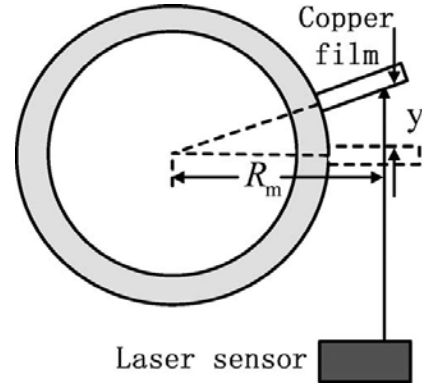


**Figure 7.** Experimental set up to measure  $\kappa$  (see [2] for additional detail).

### 2.4 Experimental Results and Model Verification

Figures 8 and 9 show the experimental results on actuation induced deformation for Sample 1. The measured value of  $\lambda_z$  was then used in conjunction with Equation (18) and the requirement  $T = 0$  to obtain theoretical values for  $r_i$  and  $\kappa$  as predicted by the nonlinear elasticity based model. Both the measured inner radius value and the measured amount of twist during the deformation are in good agreement with that predicted by the theoretical model as shown in Figures 8 and 9. Full details and additional comparisons can be found in [2].

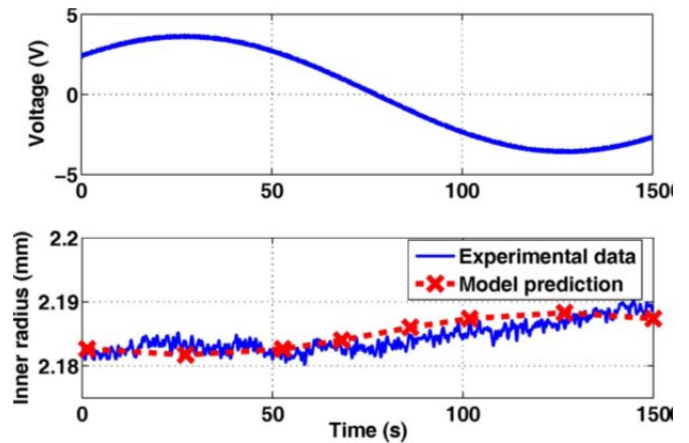


**Figure 8.** Change of inner radius  $r_i$  under a 0.005-Hz sinusoidal voltage input for Sample 1 (see [2] for additional detail).

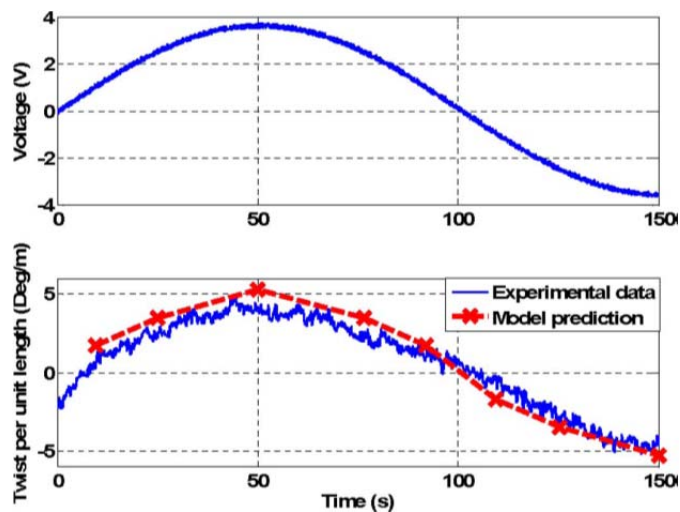


**Figure 9.** Twist per unit length  $\kappa$  under a 0.005-Hz sinusoidal voltage input for Sample 1 (see [2] for additional details).

### 3. Summary Comments

The deformation that was considered here for analysis and device validation, namely that of torsion, is only one of many that could conceivably be obtained on the basis of appropriately designed composite materials that exhibit differential swelling between the fiber and matrix constituents. In [6] and [7] the separate and relatively simpler deformation of controlled radial expansion was studied by considering the relatively more complicated geometry of a tube with two counterbalancing fiber families. More challenging are the various plant motions (such as vine twinning, petal opening, and leaf rolling) that are achieved via swelling and deswelling of plant tissue with preferentially aligned fibers ([8], [9], [10]). The determination of precise fiber geometry arrangements that can lead to such finely controlled complex deformation modes is an extremely interesting engineering issue.

### Acknowledgments

This paper was made possible by NPRP grant # 4-1333-1-214 from the Qatar National Research Fund (a member of the Qatar Foundation). The statements made herein are solely the responsibility of the authors.

### References

- [1] H. Demirkoparan and T. J. Pence. Torsional swelling of a hyperelastic tube with helically wound reinforcement. *Journal of Elasticity*, **92**: 61–90, 2008.
- [2] Y. Fang, T. J. Pence and X. Tan. Fiber-Directed Conjugated-Polymer Torsional Actuator: Nonlinear Elasticity Modeling and Experimental Validation. *IEEE/ASME Transactions on Mechatronics*, **16**(4): 656–664, 2011.
- [3] R. Baughman, Conducting polymer artificial muscles. *Synthetic Metals*, **78**: 339–353, 1996.
- [4] A. Della Santa, D. De Rossi, and A. Mazzoldi, Characterization and modelling of a conducting polymer muscle-like linear actuator. *Smart Material Structures*, **6**: 23–34, 1997.
- [5] M. Kaneko and K. Kaneto, Electrochemomechanical deformation in polyaniline and poly(o-methoxyaniline). *Synthetic Metals*, **102**: 1350–1353, 1999.
- [6] H. Demirkoparan and T. J. Pence, Swelling of an internally pressurized nonlinearly elastic tube with fiber reinforcing, *Int. J. of Solids and Structures*, **44**: 4009–4029, 2007.
- [7] H. Demirkoparan and T. J. Pence, The effect of fiber recruitment on the swelling of a pressurized anisotropic nonlinearly elastic tube, *Int. J. of Nonlinear Mechanics*, **42**: 258–270, 2007.
- [8] A. Care, L. Nefedev, B. Bonnet, B. Millet, and P. Badot, Cell elongation and revolving movement in phaseolus vulgaris l. Twining shoots, *Plant Cell Physiol.*, **39**: 914–921, 1998.
- [9] C. Lloyd and J. Chan, Microtubules and the shape of plants to come, *Nature Rev.: Mol. Cell Biol.*, **5**: 13–22, 2004.
- [10] R. Elbaum, S. Gorb, and P. Fratzl, Structures in the cell wall that enable hygroscopic movement of wheat awns, *J. Struct. Biol.*, **164**: 101–107, 2008.